Science of the Total Environment 730 (2020) 138417

Contents lists available at ScienceDirect

Science of the Total Environment

journal homepage: www.elsevier.com/locate/scitotenv

Wood-based activated biochar to eliminate organic micropollutants from biologically treated wastewater

Nikolas Hagemann [a,b], Hans-Peter Schmidt [b], Ralf Kägi [c], Marc Böhler [c], Gabriel Sigmund [a,b,d], Andreas Maccagnan [c], Christa S. McArdell [c], Thomas D. Bucheli [a,*]

[a] Agroscope, Environmental Analytics, Reckenholzstrasse 191, 8046 Zurich, Switzerland
[b] Ithaka Institute, Ancienne Eglise 9, 1974 Arbaz, Switzerland
[c] Eawag, Swiss Federal Institute of Aquatic Science and Technology, CH-8600 Dübendorf, Switzerland
[d] Department of Environmental Geosciences, University of Vienna, A-1090 Vienna, Austria

HIGHLIGHTS

- Activated biochar effectively removed organic micropollutants from real-word wastewater.
- Activated biochar from renewable sources can replace activated carbon from fossil precursors.
- Degree of activation had higher impact than quality of wood used as pyrolysis feedstock.

GRAPHICAL ABSTRACT

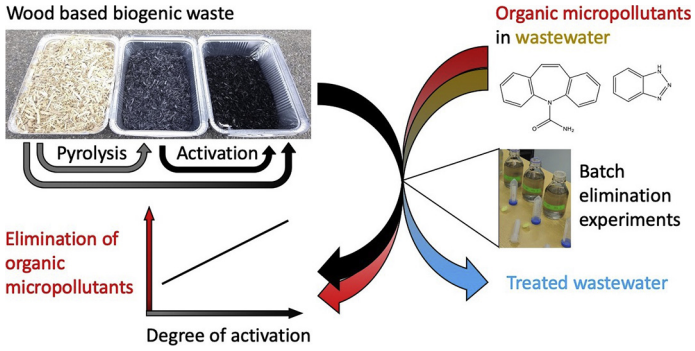

ARTICLE INFO

Article history:
Received 14 January 2020
Received in revised form 11 March 2020
Accepted 1 April 2020
Available online 28 April 2020

Editor: Daniel CW Tsang

Keywords:
Organic micropollutants
Activated carbon
Biochar
Pyrolysis physical activation
Steam activation
Quaternary wastewater treatment

ABSTRACT

Implementing advanced wastewater treatment (WWT) to eliminate organic micropollutants (OMPs) is a necessary step to protect vulnerable freshwater ecosystems and water resources. To this end, sorption of OMP by activated carbon (AC) is one viable technology among others. However, conventional AC production based on fossil precursor materials causes environmental pollution, including considerable emissions of greenhouse gases. In this study, we produced activated biochar (AB) from wood and woody residues by physical activation and evaluated their capability to eliminate OMPs in treated wastewater. Activated biochar produced under optimized conditions sorbed 15 model OMPs, of which most were dissociated at circumneutral pH, to the same or higher extent than commercial AC used as a reference. While wood quality played a minor role, the dosage of the activation agent was the main parameter controlling the capacity of ABs to eliminate OMP. Our results highlight the possibility for local production of AB from local wood or woody residues as a strategy to improve WWT avoiding negative side effects of conventional AC production.

* Corresponding author.
E-mail address: thomas.bucheli@agroscope.admin.ch (T.D. Bucheli).

https://doi.org/10.1016/j.scitotenv.2020.138417

1. Introduction

Insufficient removal of organic micropollutants (OMPs) during conventional wastewater treatment (WWT) results in their discharge into surface waters, affecting aquatic organisms and threatening (drinking) water resources (Daughton and Ruhoy, 2009; Gross et al., 2001; Hoeger et al., 2005; Sudhakaran et al., 2013). In Switzerland, selected WWT plants (WWTPs), e.g. the ones serving at least 80,000 inhabitants, have to upgrade their process with advanced water treatment until 2040 to reduce OMP discharge. For their evaluation, a representative selection of twelve OMPs have to be reduced on average by 80% from influent to effluent of a WWTP, which are known to be abundant in all Swiss wastewaters and are also known to be insufficiently removed by conventional WWT (Bourgin et al., 2018; Götz et al., 2015). Two of them (Diclofenac, Clarithromycin) are also part of the EU watch list (Decision 2015/495/EU, cf. Barbosa et al., 2016). Based on the information about the installed and planned facilities as presented by the platform "Process Engineering Micropollutants" of the Swiss Water Association (www.micropoll.ch), approximately 50% of those facilities will use activated carbon (AC) to remove OMPs. This includes powdered activated carbon (PAC) or granular activated carbon (GAC), either as standalone approach or following ozone treatment. While Switzerland has a legal commitment to upgrade their WWTPs, removal of OMP in Germany is promoted by dedicated competence centers (e.g. DWA, 2020). It is expected that similar measures will be introduced to several countries in the EU soon (Rogowska et al., 2020); as OMPs have been detected and monitored in treated wastewater all over the world (e.g. Sun et al., 2014; Zhang et al., 2008).

Assuming average AC dosages of 10–20 mg L^{-1} treated wastewater (Evers et al., 2017; Vogel et al., 2014), we estimate an annual demand of 2,500–3,500 t PAC and 700–900 t GAC for Swiss WWT. Mining of fossil precursors, the activation process and transportation of AC (Tan et al., 2017) cause the emission of considerable amounts of greenhouse gases, which are quantified as 11–18 t CO_2-equivalents t^{-1} for AC production and 2–4 t CO_2-equivalents t^{-1} for reactivation of GAC (DWA, 2016). Thus, the annual AC supply for advanced WWT in Switzerland would result in greenhouse gas emissions of 30,000–70,000 t CO_2-equivalents. Hence, replacing fossil feedstocks of AC (lignite, coal) with sustainably and locally sourced biomass combined with local production (activation) has the potential to reduce greenhouse gas emissions related to advanced WWT considerably. While the production process might still require external energy and thus would generate greenhouse gas emissions, emissions from sustainably harvested wood or wood residues are generally considered as carbon neutral. Local production e.g. in Switzerland would ensure highest standards with regard to air pollution and cut transportation-related emissions.

Biomass-based AC or *activated biochar* (AB) can be produced by pyrolysis combined with chemical or physical activation, which can further be complemented with non-thermal post-production treatments such as washing (Hagemann et al., 2018). Numerous studies are published on the production of AC from biomass and their performance as sorbents are reviewed e.g. by Devi and Saroha (2017), Dias et al. (2007), Ioannidou and Zabaniotou (2007) and Xu et al. (2015). However, poorly documented conditions of (physical) activation and data on sorption of only single OMPs from matrices with limited relevance prevent consistent data comparison, interpretation and hamper the transfer to the results to field scale operations.

Thus, we prepared ABs using a pilot-scale research pyrolysis and activation unit in a continuous (not batch) process and assessed the performance of systematically designed ABs by quantifying OMP removal from biologically treated wastewater. Although chemical activation was identified to be advantageous to produce AC for (waste)water treatment at lab scale (Kim et al., 2017; Kong et al., 2013; Wong et al., 2018), we focused on physical activation, to avoid the use of chemical activation agents and thus the production of contaminated process effluents during AB production. Also, we want to avoid the risk of leaching of residual activation agent to the wastewater during AB application in WWT. Therefore, we waived chemical modification of carbonaceous materials, too. Also, modification would increase the costs of AC production (Bhatnagar et al., 2013).

In physical activation, oxidizing gases like oxygen, steam or carbon dioxide are used to increase the surface area of a carbonaceous precursor by partial oxidation (Hagemann et al., 2018). Pyrolysis and activation was either performed as a combined one-step process, or sequentially, as a two-step process (Cagnon et al., 2003; Fu et al., 2013; Hagemann et al., 2018). We report the dosage of the activation agent (e.g. steam) quantitatively, normalized to the carbon content of the feedstock, to allow comparisons between different types of feedstock, different process parameter and also between studies. Our focus is on woody feedstocks for pyrolysis and activation, due to their ubiquity in Switzerland. We hypothesized that AB from these resources can remove OMPs to the same or higher extent as commercially available ACs based on fossil precursors.

2. Materials and methods

2.1. Feedstock sourcing and preparation

Beech wood with bark, pine and fir without bark, coniferous bark and landscaping wood were provided by ZürichHolz AG (Wetzikon ZH, Switzerland). Bark was sieved to <20 mm by the supplier and used as obtained, as further sieving was not useful due to the specific texture of bark. Pre-chopped wood was sieved either to 2–4 mm or 4–8 mm. Compost residual wood and waste timber were provided by Oberland Energie AG (Thun, Switzerland), processed with a garden shredder and a cutting mill (20 mm sieve, Retsch, Haan, Germany), and sieved to 4–8 mm. Mixed wood chips from both coniferous and deciduous trees were collected from a bunker of a central heating. After processing in a cutting mill with a 20 mm sieve, we used the two sieving fractions 2–4 mm and 4–8 mm.

2.2. Activated carbon and non-activated biochar used as benchmark sorbents

Activated carbon "Carbopal AP" (Donaucarbon, Frankfurt, Germany) produced from lignite coal was used as a commercially available reference AC. Activated carbon "Norit SAE Super" (Cabot Corporation, SIA Cabot Latvia, Riga, Latvia) produced from mixed feedstock was used as a second commercial reference for additional elimination batch experiments with selected sorbents. Carbonized wood and plum stones produced through flame curtain pyrolysis (Cornelissen et al., 2016; Schmidt and Taylor, 2014), and char from wood gasification (Syncraft process, Huber, 2010) were kindly provided by Basna d.o.o. (Čačak, Serbia), and Energiewerk Ilg GmbH (Dornbirn, Austria), respectively.

2.3. Production of activated biochar

Thermal conversion of biomass was performed in one or two steps on a PYREKA research pyrolysis and activation unit (Pyreg GmbH, Dörth, Germany, Fig. 1). Feedstock was placed in the feeder from where it was transported by an auger into a rotary feeder separating the thermal reactor from the environment. The reactor was a 1 m long tube where an auger transports the feedstock within 10 min (or any longer time) from one end to the other. If not mentioned otherwise, the reactor was electrically heated to 900 °C and a residence time of 10 min was used. This temperature was selected because physical activation with steam or CO_2 requires temperatures higher than 850 °C (Marsh and Reinoso, 2006), and Yang et al. (2010) produced ABs with the highest specific surface area at 900 °C when testing an activation temperature range of 750–950 °C. Also, Yu et al. (2019) did not find an increase in specific spesurface area when using CO_2 instead of N_2 as purge gas during pyrolysis at 750 °C, while Wan et al. (2019) found 5-

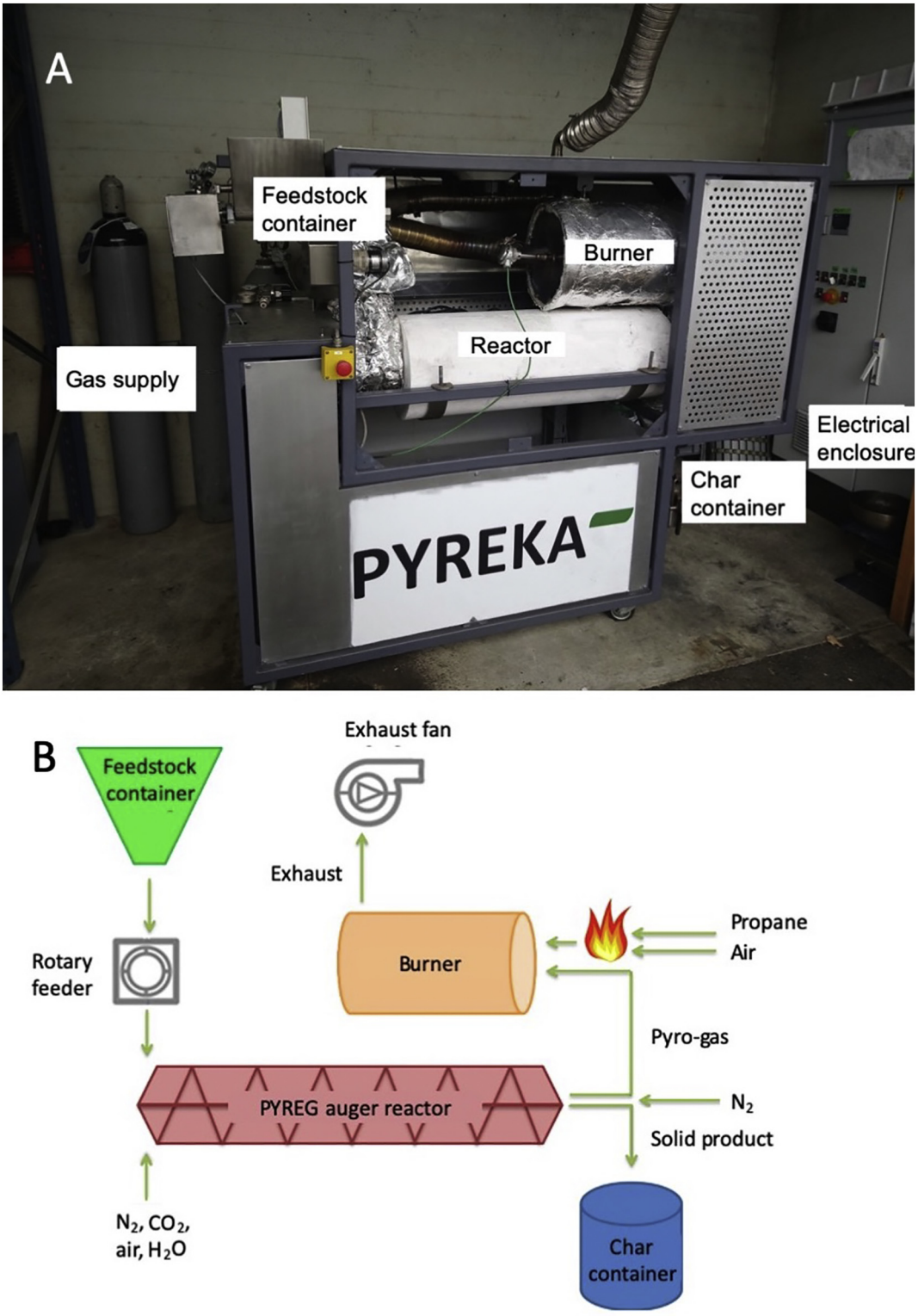

Fig. 1. PYREKA research pyrolysis unit (A) and its flow chart adapted from the manual provided by the manufacturer (B). The reactor is 1 m long and heated electrically. An auger in the feedstock container doses the feedstock onto a rotary feeder just above the reactor. Gas and/or water vapor are injected right at the beginning of the reactor (left end). After being transported from left to right through the reactor by an auger, the solid product drops into the char container, while the gases are sucked into the burner without prior separation of the liquid fraction. N_2 is injected just above the char container to ensure that pyro-gas does not concentrate in the char container.

fold increase of SSA when using CO_2 instead of N_2 at 900 °C. At the end of the reactor, the biochar or AB was discharged into a cooled and air-tight container. The discharge tube above this container was heated to 400 °C and flushed with 2 L min^{-1} N_2 to reduce re-condensation of volatiles on the solid pyrolysis/activation product. The syngas was combusted in a separate burning chamber.

Dosage of the feedstock was controlled through velocity of the auger of the feeder. For each feedstock, the specific feeding rate was determined during cold operation of the PYREKA for 2 h, when the amount of feedstock transported through the machine was measured in intervals of one to ten minutes. The feeding rate was then adjusted to 600 g h^{-1} for wood and 200 g h^{-1} for biochar (in case of a two-step

activation process). Depending on the pourability of individual feedstock batches, the feeding rate may have varied by ±20% (Fig. S1).

For steam activation, the required amount of deionized water was dosed with a peristaltic pump into a stream of 2 L min^{-1} N_2 and was converted to steam in the tube by the excess heat of the reactor. For activation with CO_2, CO_2 + steam, air, steam + air, the required amount of gas was supplied with flow rates of 2–10 L min^{-1} in absence of additional N_2. The gas inlet was located at the downspout between the rotary feeder and the auger of the thermal reactor. The dosage of oxidizing agents (CO_2, O_2 in air, steam) was calculated to achieve a defined molar ratio of oxidizing agent to carbon in the feedstock.

In addition to one-step activation in which the feedstock is directly exposed to the conditions of activation (high temperature, oxidizing environment), we also tested two-step activation. For that purpose, mixed wood as well as pine and fir wood were first pyrolyzed at 600 °C in an inert environment (by flushing only with 2 L min^{-1} N_2). After cooling down, the resulting biochar was activated with steam for 10 min at 900 °C. Both steps were performed sequentially in the PYREKA.

Each individual sample of biochar or AB was produced for at least three reactor volumes under constant conditions (feedstock, residence time, temperature, gases), e.g. for 30 min if residence time was 10 min. Between the production of two samples of the same type of feedstock, the production of three reactor volumes was discarded to ensure a clear separation of the samples obtained under different production parameters. Between the production of two samples from different type of feedstock, it was assured that the reaction tube was emptied, and new feedstock was supplied for at least five reactor volumes to ensure homogenous supply and an even distribution of the feedstock throughout the reactor. Yields were calculated by dividing the mass of biochar/AB produced per unit of time by the feeding rate. Feedstock and conditions of production for all sorbents used for the elimination experiments are specified in Table 1.

Biochar produced from pine and fir wood at 600 °C, and AB produced from the same type of wood (ID 21, cf. Table 1), respectively, were washed with water, aqueous NaOH solution, hydrochloric acid and ethanol. A total of twelve different combinations of these solvents as detailed in the SI (Table S2) were applied to evaluate to what extent an additional washing procedure improved the sorption capacity of the AB.

2.4. Characterization of sorbents

Analyses were performed after milling to <200 μm with an impact mill (Retsch, Haan, Germany) in a fume hood. Elemental analysis (CHO) was performed on a Euro EA 3000 (Hekatech, Germany). Gas adsorption with N_2 and CO_2 to quantify specific surface area (SSA) and pore volume (PV) was performed on a Nova 2000 (Quantachrome Instruments, Boynton Beach, FL, USA) after degassing at 40 °C for 18 h (Bachmann et al., 2016; Hagemann et al., 2017; Sigmund et al., 2017). The particle size distributions for sorbent suspensions in treated wastewater were determined using laser shading with an EyeTech particle size and shape analyzer (Ambivalue, Dussen, The Netherlands, Table S3). The electrophoretic mobility of particles remaining in suspension in treated wastewater and ultrapure water after a settling period of 1 h was measured on a ZetaSizer Nano ZS (Malvern Instruments Ltd., UK, Table S3.)

Table 1
Feedstock, parameters of production, yield and elemental composition (CHO) of (activated) biochars used for screening experiments. IDs in bold indicate sorbents additionally used for experiments with OMP quantification (Sections 3.2 and 3.3).

ID	Feedstock	Feedstock	Thermal treatment		Activation agent		Yield[c]	Sorbent elemental composition				Sorbent ζ potential	
		Particle size	HTT[a]	Duration	Type	Molar ratio[b]		C content	H/C ratio	O/C ratio	BET SSA	Treated WW[f]	MilliQ[g]
		[mm]	[°C]	[min]			[mass%]	[mass%]			[$m^2 g^{-1}$]	[mV]	[mV]
1	Mixed wood	4–8	750	10	None	n.a.	20 ± 2%	91.1	0.14	0.030	n.d.	n.d.	n.d.
2	Mixed wood	4–8	900	10	None	n.a.	19 ± 2%	94.3	<LOD[d]	0.022	n.d.	n.d.	n.d.
3	Wood (Kon-Tiki)	n/a	~650	~4–6 h	None	n.a.	n.d.	83.7	0.16	0.039	n.d.	n.d.	n.d.
4	Plum stones (Kon-Tiki)	n/a	~650	~4–6 h	None	n.a.	n.d.	82.7	0.30	0.041	n.d.	n.d.	n.d.
5	Wood (gasifier)	n/a	~800	h – days	None	n.a.	n.d.	75.2	<LOD[d]	0.031	n.d.	n.d.	n.d.
6	Mixed wood	2–4	900	10	Steam	0.50	11 ± 1%	85.0	0.06	0.038	n.d.	n.d.	n.d.
7	Mixed wood	2–4	900	10	Steam + O_2	0.50 + 0.10	9 ± 1%	83.9	0.06	0.039	n.d.	n.d.	n.d.
8	Mixed wood	2–4	900	10	Steam + CO_2	0.50 + 0.50	8 ± 1%	77.2	0.06	0.055	n.d.	n.d.	n.d.
9	Mixed wood	2–4	900	10	Steam	1.00	8 ± 1%	77.9	<LOD[d]	0.053	826	−8.7 ± 1.0	−12.5 ± 0.6
10	Mixed wood	4–8	900	10	Steam + CO_2	0.50 + 0.50	13 ± 2%	91.8	<LOD[d]	0.029	n.d.	n.d.	n.d.
11	Mixed wood	2–4	900	20	Steam + CO_2	0.50 + 0.50	15 ± 2%	84.2	0.06	0.036	n.d.	n.d.	n.d.
12	Beech wood	4–8	900	10	None (N_2)	n.a.	14 ± 1%	91.0	<LOD[d]	0.022	345	−8.6 ± 0.7	−20.0 ± 1.3
13	Beech wood	4–8	900	10	Steam	0.33	8 ± 0%	94.7	<LOD[d]	0.023	n.d.	n.d.	n.d.
14	Beech wood	4–8	900	10	Steam	0.50	6 ± 0%	90.3	<LOD[d]	0.029	780	−7.9 ± 1.0	−12.3 ± 0.2
15	Beech wood	4–8	900	10	Steam	1.00	2 ± 0%	78.6	<LOD[d]	0.059	913	−7.8 ± 1.0	−16.2 ± 0.7
16	Beech wood	4–8	900	10	Steam + CO_2	0.50 + 0.50	4 ± 0%	84.1	<LOD[d]	0.047	899	−8.3 ± 1.2	−15.0 ± 1.0
17	Coniferous bark	< 20	900	10	Steam	0.50	17 ± 0%	81.4	<LOD[d]	0.041	549	−8.3 ± 0.9	−13.3 ± 0.6
18	Woody landscaping residues	4–8	900	10	Steam	0.50	7 ± 0%	83.0	<LOD[d]	0.052	n.d.	n.d.	n.d.
19	Compost wood	4–8	900	10	Steam	0.50	9 ± 1%	74.2	<LOD[d]	0.071	945	−8.9 ± 0.7	−22.8 ± 0.7
20	Waste timber	4–8	900	10	Steam + CO_2	0.50 + 0.50	8 ± 0%	94.1	<LOD[d]	0.018	n.d.	n.d.	n.d.
21	Pine and fir w/o bark	4–8	900	10	Steam	1.00	5 ± 0%	92.1	<LOD[d]	0.019	1235	−8.3 ± 1.3	−11.9 ± 1.8
22	Mixed wood biochar - 600°C[e]	n/a	300	10	O_2	0.25	n.d.	83.6	0.26	0.065	n.d.	n.d.	n.d.
23	Mixed wood biochar - 600°C[e]	n/a	300	10	O_2	0.40	n.d.	81.9	0.26	0.073	n.d.	n.d.	n.d.
24	Mixed wood biochar - 600°C[e]	n/a	900	10	Steam	0.50	n.d.	86.9	<LOD[d]	0.029	n.d.	n.d.	n.d.
25	Pine and fir biochar - 600°C[e]	n/a	300	10	O_2	0.50	n.d.	85.2	0.28	0.069	n.d.	n.d.	n.d.
26	Pine and fir biochar - 600°C[e]	n/a	900	10	Steam	0.50	n.d.	85.7	<LOD[d]	0.026	741	−8.8 ± 0.7	−11.7 ± 0.9

n.a.: not applicable. n.d.: not determined.
[a] HTT = highest treatment temperature during thermal conversion.
[b] Molar ratio of the oxidizing agent to the carbon content of the feedstock.
[c] Data provided as biochar yield ± standard deviation of feedstock feeding rate quantified in 10 min intervals.
[d] Level of H was below the limit of detection (LOD).
[e] Two-step activation: wood was first pyrolyzed at 600 °C for 10 min, then activated as described.
[f] Wastewater.
[g] Ultrapure water.

2.5. Elimination batch experiments

Biologically treated wastewater was obtained from WWTP Zurich Werdhölzli. This WWTP treats wastewater of 670,000 people equivalent with a dry weather flow of 0.26×10^6 m^3 day^{-1} and consists of a primary clarifier, a conventional activated sludge treatment and a deep bed sand filtration. Phosphorous is eliminated using Fe(II). Grab samples were collected between 17.07.2017 and 30.10.2017 after the secondary clarifier but prior to the sand filtration. Within 1 h after sampling, water was filtered to 100 μm with a nylon filter bag (Causabag, Infiltec GmbH, Speyer, Germany). Schott bottles (0.5 L) with Teflon seals were filled with 500 mL water.

Sorbents (Table 1) were weighted into tin capsules (5 mm × 9 mm, Huberlab, Aesch, Switzerland) that were placed into the filled Schott bottles. Bottles with control treatments without AC/AB received an empty tin capsule as blank. Bottles were closed and placed on a rotary shaker. This procedure allowed the exact dosage by using a precision scale and an almost simultaneous start of all the sorption batch experiments. After shaking for 24 h, aliquots were filtered to 0.45 μm using syringe filters (mixed cellulose ester, Chromafil A-45/25, Macherey-Nagel, rinsed with 30 mL MilliQ water prior to use, cf. Böhler, 2019), which took approximately 15–20 min from the first to the last sample within an experiment.

All sorbents were tested in triplicates in elimination batch experiments performed at 10 mg L^{-1} (±10%). UV photometry (absorbance at $\lambda = 254$ nm) was used to approximate the OMP removal (Boehler et al., 2012).

Selected sorbents (ID 9, 12, 14–17, 19, 21, 26, cf. Table 1) were additionally tested at 3.5, 7.0 and 14.0 mg L^{-1} (±3%) without replicates. Here, we combined UV photometry, quantification of dissolved organic carbon (DOC) and the quantification of 15 OMPs using liquid chromatography–mass spectrometry (LC-MS). While UV absorbance and DOC were quantified immediately after filtration, samples for LC-MS (50 mL) were stored at −20 °C until the analysis was performed.

2.6. UV and DOC measurements

UV absorbance was determined in 10 mm cuvettes at 254 nm. MilliQ water was used as a reference (0 absorbance). Reduction of UV absorbance was calculated based on the ratio of UV absorbance of the respective treatment and the average of three non-amended controls. DOC was quantified on a TOC-L (Shimadzu, Kyōto, Japan).

2.7. Quantification of micropollutants

Fifteen OMP known to be only partly removed in conventional WWT (Bourgin et al., 2018; Götz et al., 2015) were selected for quantification in the real-world wastewater used in the batch sorption experiments. The investigated compounds were natively present in concentrations ranging from 10 to 4000 ng L^{-1} (Table S6) and were: the anticorrosives 4/5-methylbenzotriazole and benzotriazole, the pharmaceuticals amisulpride, candesartan, carbamazepine, citalopram, clarithromycin, diclofenac, hydrochlorothiazide, irbesartan, metoprolol, venlafaxine, sulfamethoxazole and its human metabolite N4-acetylsulfamethoxazole, as well as the biocide mecoprop (for more details see Table S4). This list includes the twelve OMPs used in Swiss legislation, which were complemented by mecoprop, sulfamethoxazole and N4-Acetylsulfamethoxazole. For all compounds, labeled internal standards were used for quality assurance (see Table S5 for details).

After thawing the samples at room temperature for 6 h, samples were vigorously shaken. After 10 min settling, 1000 μL supernatant was transferred into a 1.5 mL sample vial and spiked with internal standards. Large volume direct injection of a 100 μL sample was thereafter performed on an Agilent 1290 HPLC equipped with an Acquity HSS T3 column (Waters) for chromatographic separation coupled to a triple quadrupole MS (Agilent TQ6495A) for detection. For quality control, two transitions and retention time deviation were recorded (see Text S1 in the SI for details). The average relative recoveries of the compounds ranged from 93% to 106%, and limits of quantification (LOQ) were between 0.6 and 2.5 ng L^{-1}, except for benzotriazole with an LOQ of 30 ng L^{-1} due to higher calibration levels as higher concentrations in the samples were expected (see Table S6 for details).

To check for the stability of OMP and their potential sorption to the syringe filter, triplicates of the coarsely filtered wastewater (100 μm) were analyzed with and without fine filtration (0.45 μm) at time zero and filtered samples also after 24 h. All nine samples showed a variability of <8%.

2.8. Distribution coefficients and poly-parameter linear free energy relationships (pp-LFER)

Distribution coefficients K_D (L kg^{-1}) of any of the 15 OMPs were calculated as.

$$K_D = C_S \, C_W{}^{-1} \quad (1)$$

where the aqueous concentration C_W (μg L^{-1}) was measured as described above, and the sorbed concentration C_S (μg kg^{-1}) was determined from mass balance calculations based on dry matter of the sorbent. Additionally, distribution coefficients K_{SA} (L m^{-2}) were calculated using the sorbed concentration of OMP based on sorbent SSA calculated according to the Brunauer-Emmett-Teller-theory (BET, Brunauer et al., 1938).

$$K_{SA} = C_{BET} \, C_W{}^{-1} \quad (2)$$

where C_{BET} is the sorbed concentration of OMP based on BET SSA (μg m^{-2}). All distribution coefficients presented were calculated as the average of three individual distribution coefficients (hence assuming a linear sorption isotherm over the relatively narrow concentration range) based on three concentrations of sorbent covering the typically applied range in WWTP (see Section 2.5). For compounds that were predominantly neutral under the experimental conditions, poly-parameter linear free energy relationships (pp-LFER) were applied using Abraham parameters from the UFZ-LSER database (Ulrich et al., 2017).

3. Results and discussion

3.1. Yield and elemental composition of biochars and ABs

A total of 24 non-activated biochars and ABs were produced with the PYREKA, three additionally supplied biochars were produced externally. The materials had a carbon, oxygen, and hydrogen content of 74–95%, 2.2–8.0% and 0.0–1.8%, respectively (Table 1). For non-activated biochars, yields as well as H/C and O/C ratio were lower at 900 °C compared to 750 °C while C content was higher at 900 °C (Table 1: ID 1 vs. 2 for mixed wood), which is in line with textbook knowledge (Krull et al., 2009).

Activation decreased the yield compared to pyrolysis without activation agent performed at the same temperature (Table 1: ID 1, 2 vs. 6). Yields decreased with increasing molar ratio of activation agent to feedstock-C (IDs 12–15). Pure steam activation resulted in lower yields compared to steam + CO_2 (1:1 ratio) activation (ID 15 vs. 16). In line with this, all ABs derived from mixed wood showed lower yields and lower C-content compared to the biochar produced from the same feedstock at the same temperature (ID 6–11 vs. 2). Low yields (<5%, Table 1) at high molar ratios of the activation agent were reported before (e.g. Yang et al., 2010).

For beech wood, the O/C ratio increased with increasing molar ratios of the activation agent, while the carbon content was increased at a low molar ratio (0.33) but decreased for activation ratios higher than 0.5

compared to the non-activated biochar (Table 1, Fig. S3). This was also observed for mixed wood and can be rationalized by three different mechanisms of activation: (1) Carbon is oxidized by the activation agent and transferred from the solid to the gas phase as CO and/or CO_2 (Hagemann et al., 2018). This may reduce C content of the product, as the inorganic matter (wood ash) remains in the solid. (2) At low dosages of the activation agent, the carbon content might increase due to the oxidation of volatiles contained in the biochar (Cagnon et al., 2003), i.e. secondary char that is trapped in biochar's pores and that may have a lower carbon content than the residual AB. (3) Carbon is oxidized but remains in its solid matrix, e.g. as ethers as was evidenced by XPS (Zhang et al., 2014), which may increase O/C ratios, although Zhang et al. could not confirm this by elemental analysis.

Yield of AB from coniferous bark (17%, Table 1, ID 17) was higher than those of wood-based AB (2–15%). Still, low H/C and O/C ratios confirmed a complete thermal conversion, despite the higher particle size of the feedstock. High yield can probably be explained by the high ash content of the feedstock (2.5–5.0%), which was 5–25 times higher than of bark free wood (Baum et al., 2001). Still, AB from bark had a carbon content of 81%, which might be the result of catalytic char formation in the presence of ash (Buss et al., 2019; Kleen and Gellerstedt, 1995). Potassium was identified as an important catalyst within the ash (Masek et al., 2019); wood and bark ash contain about 3% K as K_2O (LfU, 2020). Using ash or potassium to increase the yield of AB production needs further investigation, as this effect, to the best of our knowledge, has so far only been utilized for non-activated biochar production.

In the EU, commercially produced AC must have a carbon content of 80% or higher (ACC, 2018a, 2018b). Among the sorbents tested here, gasifier biochar (ID 5), AB from mixed wood and beech produced at high dosage of activation agent (molar ratio = 1, ID 8, 9, 15) and AB from compost wood (molar ratio = 0.5, ID 19) did not meet this 80% threshold. Still, these ABs (ID 8, 9, 15, 19) can compete with commercial AC in regard to OMP elimination as discussed in detail below.

3.2. Screening of ABs for OMP elimination

The performance of all biochars and AB in Table 1 was evaluated in several elimination experiments at 10 mg L^{-1} corresponding to a specific PAC dosage of 1.6–2.5 mg PAC mg^{-1} DOC, depending on the DOC concentrations of the treated wastewater sampled (4.1–6.4 mg L^{-1} DOC, Table S1). The reduction of UV absorbance at a wavelength of 254 nm can be used as surrogate for the elimination of OMPs (Zietzschmann et al., 2014), as will be shown later. For the Carbopal AP reference material, the reduction of UV absorbance was on average 23 ± 1% (average ± standard deviation, $N = 8$, Fig. 2, Table S1).

Reduction of UV absorbance by non-activated biochars was one order of magnitude lower than of Carbopal AP (Fig. 2A), which corresponds to the findings of e.g. Nair and Vinu (2016), who found that non-activated biochar could barely eliminate model contaminants from water. Thus, non-activated, wood-based biochars, which had considerably higher yields than AB, are not suited for OMP elimination in advanced WWT.

Using AB generally resulted in similar or higher reduction of UV absorbance compared to the treatment with Carbopal AP (Fig. 2B–F). Mixed wood was converted into an AB equally effective as Carbopal AP when treated with steam at a H_2O to C molar ratio of 0.5 (ID 6). When O_2 or CO_2 (ID 7, 8) were mixed with the same amount of steam as additional oxidizing agent, or when the amount of steam was doubled (molar ratio of H_2O to C = 1, ID 9), even more efficient sorbents were produced (Fig. 2B). However, this reduced AB yield from 11 ± 1% to 8–9% (Table 1). This highlights the importance for future studies to describe the dosage of oxidizing agents in physical activation in a quantitative manner, i.e. as a molar ratio, which seems to be missing in many studies (cf. papers reviewed by Ioannidou and Zabaniotou, 2007) or is reported insufficiently, e.g., referring to flow rates but not mentioning the amount of feedstock treated. Also, to evaluate the suitability of a certain feedstock for AB production, several molar ratios of oxidation agent to feedstock carbon should be tested to find an optimal dosage. Yang et al. (2010) showed that the activation of coconut shells by CO_2 in a one step process at 900 °C for 2 h resulted in the highest BET surface area when CO_2 flow rates of 200–400 mL min^{-1} were combined with 30 g feedstock, i.e. a molar ratio of 1–2 was applied. Both lower and higher flow rates resulted in lower SSA. However, neither Yang et al. (2010) nor our study controlled whether the oxidizing agent reacted completely during the activation process, or if residual CO_2, or H_2O, was present in the exhaust.

To evaluate the impact of the intensity of the thermal treatment, which is both a function of residence time and feedstock particles size, we used two different particle sizes of the feedstock and two different residence times (Fig. 2C). Increasing the intensity of the thermal treatment by using smaller particle size (2–4 mm vs. 4–8 mm) of the feedstock (i.e. faster heat transfer from the outside of a particle to its core) increased the reduction of UV absorbance from 21% to 37% (ID 10 vs 8) while decreasing both yield and carbon content of the AB (Table 1). Doubling the residence time while using the smaller particle size to further increase intensity (ID 11) led to a decrease of the performance (from 37% to 25% reduction of UV absorbance), while the yield of AB was similar. Hence, a residence time of 10 min and a feedstock particle size of 2–4 mm was identified as the optimal conditions for producing AB from mixed wood in PYREKA. This residence time is considerably shorter than those reported in the literature, including values of 1–2 h (Ioannidou and Zabaniotou, 2007) or even up to 15 h (Cao et al., 2001) and/or finer particle sizes (e.g. <200 μm, Cagnon et al., 2003) when AC/AB were produced in batch processes in muffle, tube or similar furnaces, in which the feedstock was not moved, and exposed to a steady heating rate. In the PYREKA, the feedstock is immediately exposed to the final pyrolysis and/or activation temperature just after passing the rotary feeder, and thus shorter residence times resulted in highly carbonized materials. Additionally, feedstock movement through the auger further promoted a homogenous process, quicker inner particle heating rates and an intense interaction with the gas phase.

Having optimized the intensity of the thermal treatment, we focused on the activation agent. Using beech wood, a higher dosage of steam resulted in ABs showing a higher reduction of UV absorbance, within the range of 0.33–1 for the molar ratio of H_2O to feedstock-C (ID 12–15, Fig. 2D). However, as described above for mixed wood, higher dosage of steam also results in lower yields (Table 1, Fig. S3), which highlights the trade-off in the production of AB. Thus, an optimum "elimination per unit of feedstock" needs to be identified for each type of feedstock. Additionally, higher dosage of steam decreased the carbon content to <80% while O/C increased with increasing dosage of steam (Table 1, Fig. S3), indicating an increase of carbon functional groups. As for mixed wood, AB from activation with a mixture of steam and CO_2 (ID 16) showed similar reduction of UV absorbance when compared to a steam-only activation performed with the same molar ratio (ID 15). Remarkably, both AB yield and C content were higher when CO_2 was used (Table 1), which makes the addition of CO_2, e.g. recycled from the exhaust, to the activation reactor an interesting option to perform activation.

We then compared different types of wood used as feedstock (Fig. 2E). Low cost wood residues from landscaping (ID 18), compost residual wood (ID 19) and waste timber (ID 20, shredded furniture, wood from demolition works, etc.) were all suitable feedstock for AB production. Resulting ABs were able to reduce UV absorbance by 30–35% at 10 mg L^{-1}, which is a higher reduction than achieved with Carbopal AP (23 ± 1%). Still, ABs based on pure wood obtained from forestry (beech – ID15, pine and fir – ID 21) outperformed ABs based on residues with reduction rates of 41% for both AB. Both from an ecological and economic perspective (price of feedstock), however, the use of residues would probably be advantageous. In Switzerland, about one million tons of waste timber need to be disposed annually, of which 17% are

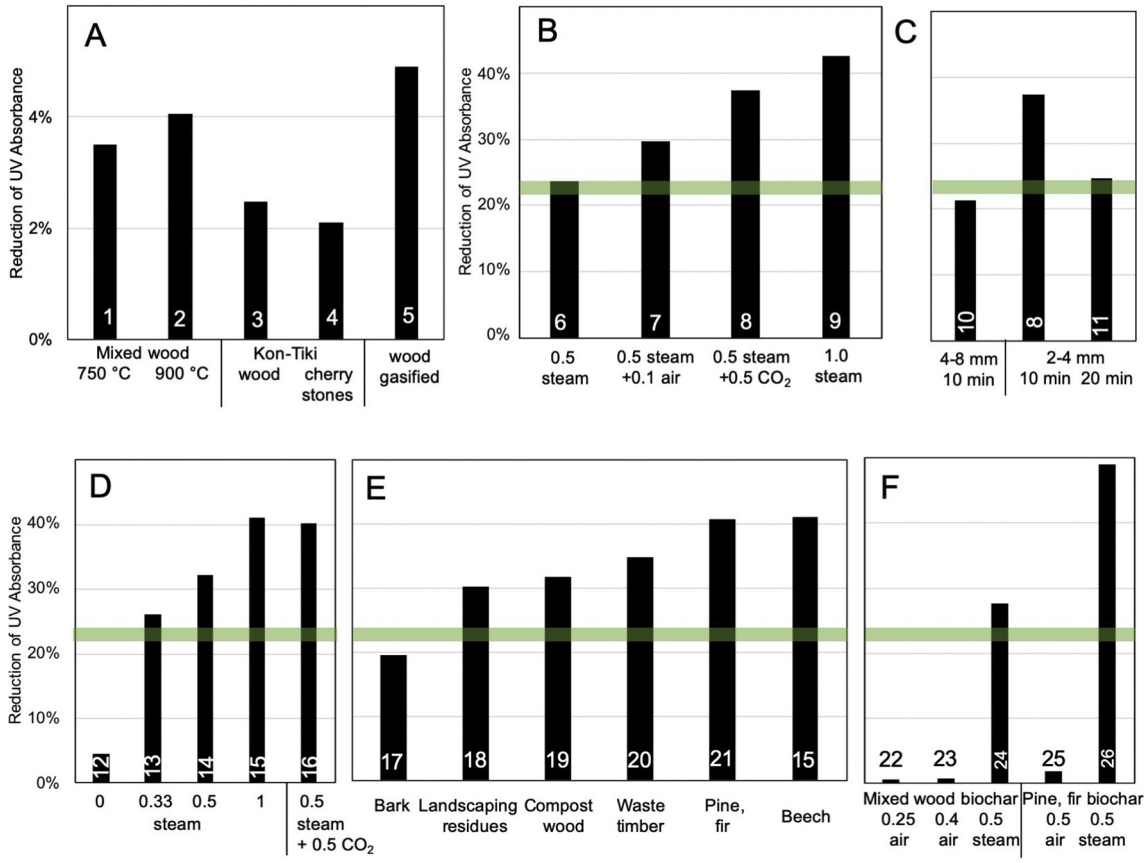

Fig. 2. Screening of organic micropollutant elimination by reduction of UV absorbance (254 nm) in treated wastewater of WWTP Zurich Werdhölzli after shaking for 24 h with 10 mg L^{-1} sorbent. Different panels show tests of different aspects (bold text) of biochar activation: A: **Non-activated biochars** produced from mixed wood and three commercial biochars. B: **Activation agent**: Activated Biochar (AB) produced from mixed wood sieved to 2–4 mm using different gas mixtures at different molar ratios of activation agent to feedstock carbon. C: **Intensity**: AB produced from mixed wood with steam and CO_2, each applied at a molar ratio of 0.5, with increasing intensity of the thermal conversion by reducing feedstock particle size and increasing duration of the thermal treatment. D: **Degree of activation**: Beech wood ABs produced with increasing degrees of activation achieved by increasing molar ratio of steam. At molar ratio of 1, we additionally tested activation with CO_2 + steam (1:1). E: **Feedstock quality**: AB produced from different feedstock. F: AB produced by pyrolysis and activation performed as a **2-step process** with the PYREKA. Mixed wood as well as pine and fir were first pyrolyzed for 10 min at 600 °C to obtain a biochar. In a second run, activation was performed at 300 °C with air ("post pyrolysis air oxidation", Xiao and Pignatello, 2016) or at 900 °C with steam. Green, horizontal bars indicate the average reduction of UV absorbance by a commercial AC (Carbopal AP) throughout eight sorption batch experiments as a reference (cf. Table S1). Detailed information on each sorbent are displayed in Table 1 using the numbers in or above the bars as the ID. Error bars are not shown, as triplicate sorption batch experiments showed a variation of <3% of the average.

exported (Erni et al., 2017). Based on a mass yield of 8% (Table 1) about 13,600 t of AB could be produced from the waste timber that is exported today - that is, approximately three times the demand we calculated for advanced wastewater treatment. Sørmo et al. (2020) performed waste timber pyrolysis on a medium-scale pyrolysis unit (750 t yr^{-1}) and found that gaseous emission factors of various pollutants (emissions per amount of biochar produced) for waste timber were similar or even lower than for clean wood with leaves. However, organic and inorganic pollutants in the biochar need to be monitored carefully, as they were found to accumulate in the solid product.

With 20% UV-reduction, AB based on coniferous bark (ID 17), which is e.g. a residue of sawmills, was slightly less effective in reducing UV absorbance compared to Carbopal AP (Fig. 2E). Nevertheless, bark should be looked at as an interesting source for AB feedstock, as there are currently only few competing applications, unlike for landscaping residues and waste timber, which are often used as fuel in biomass power plants. Also, bark typically does not contain any artefacts or stones that would require further processing, unlike e.g. compost wood that may contain stones as well as metal or polymer artefacts that hinder its direct pyrolysis.

Two-step activation of the biochar obtained from pyrolysis at 600 °C was performed with steam (900 °C, 10 min, H_2O to C = 0.5, ID 24 and 26) and resulted in ABs that reduced UV absorbance to a comparable degree as those produced in the one-step process (28% vs. 24–42% for mixed wood, cf. Fig. 2F, B, 49% vs. 42%, cf. Fig. 2F, E). Treating (non-activated) biochar at 300 °C with air for 10 min (ID 22–23, "post pyrolysis air oxidation", Xiao and Pignatello, 2016) did not result in ABs performing beyond the capacities of the original biochar. Xiao and Pignatello (2016) showed that post-pyrolysis air oxidation eliminates volatiles from the char surface and increases carboxylic groups on the biochar surface, resulting in improved sorption of selected organic molecules, both neutral compounds and ionizable weak acids and weak bases, from an aqueous solution due to pore reaming and the promotion of charge-assisted hydrogen bonding. However, a commercial AC reference still outperformed biochars after post-pyrolysis air activation (Xiao and Pignatello, 2016), which is in line with our data. Washing of both, biochar and AB, applied as a post-production treatment to improve their sorption capacity barely affected the reduction UV absorbance of these materials (Table S2, Fig. S3).

3.3. Elimination of DOC and OMP by selected sorbents

We selected the best performing ABs based on the semi-quantitative approach of UV absorbance reduction (chapter 3.1.2) for further in-depth investigations. Specifically, we chose three beech wood ABs (ID 14–16) complemented by a non-activated beech wood biochar (ID 12), two pine and fir ABs (ID 21 and 26) as well as ABs based on composted wood (ID 19), bark (ID 17) and mixed wood (ID 9,

Table 1). In addition to Carbopal AP, we used Norit SAE Super as an additional reference material.

The DOC elimination and the average elimination of all 15 OMPs by the experimental ABs were comparable to the corresponding elimination observed for the two reference ACs (Fig. 3A). As expected, the non-activated biochar did not perform well. A good correlation between the reduction of UV absorbance and DOC elimination, as well as between UV absorbance and OMP elimination was found for all evaluated sorbents in wastewater from WWTP Zurich Werdhölzli (Fig. 3). Specifically, we found a linear correlation ($R^2 = 0.98$) for UV absorbance vs. DOC (Fig. 3B). This is in good agreement with previous studies and shows that there is overall no preferential sorption of organic compounds with unsaturated bonds that absorb UV light (Dobbs et al., 1972). A good correlation of UV absorbance vs. OMP (average of elimination of 15 OMPs) was also found but was linear only for UV absorbance reductions < 20% ($R^2 = 0.96$), which includes average OMP elimination of up to 60% (Fig. 3C). Thus, ABs and ACs preferentially eliminate OMP compared to bulk DOC. Overall, these results confirm the suitability of using UV absorbance as a quick and easy screening method to assess the suitability of AC/AB for advanced WWT (Boehler et al., 2012; Zietzschmann et al., 2014).

3.4. OMP sorption by selected sorbents

While elimination in terms of residual concentration reduction is the key parameter to test the suitability of a given sorbent for its application in a WWTP, solid-water phase distribution coefficients K_Ds are commonly used to investigate sorption processes. In our case, elimination data can be translated into mass or surface area normalized K_Ds via three-point sorption isotherms presented in the SI (Figs. S4–S18).

3.4.1. Impact of sorbate properties

Of the OMPs investigated, 14 out of 15 contained ionizable functional groups. Speciation of ionizable sorbates (Table S4) is an important property that affects their sorption to AC and AB (Kah et al., 2017; Kovalova et al., 2013). At circum-neutral pH of Zurich Werdhölzli treated wastewater, four compounds were predominantly neutral (5-methylbenzotriazole, benzotriazole, carbamazepine, hydrochlorothiazide), five compounds were predominantly cationic (amisulpride, citalopram, clarithromycin, metoprolol, venlafaxine) and six compounds were predominantly anionic (candesartan, diclofenac, irbesartan, mecoprop, N4-acetylsulfamethoxazole, sulfamethoxazole; Table S4). Anionic compounds can be electrostatically repulsed from negatively charged or polar oxygen containing functional groups on the AC or AB surfaces, whereas cationic compounds can be electrostatically attracted to these functional groups (Kah et al., 2017). However, in our data set, charge interactions lost relevance once hydrophobicity dominated. To differentiate hydrophobic and non-hydrophobic interactions, we used the pH dependent lipophilicity proxy log D (Schwarzenbach et al., 2017, Table S4). For hydrophobic compounds with log D > 1, hydrophobic partitioning can explain that K_D was within the same range for all those compounds, irrespective of their charge (Fig. 4A). For OMP with low hydrophobicity (log D < 1, Table S4), cationic compounds had higher K_D than neutral compounds while lowest K_D were observed for anionic compounds (Fig. 4A). However, OMPs in treated wastewater comprise thousands of different substances and our selection of 15 substances did not aim to be representative with regard to sorbate properties. For instance, Kovalova et al. (2013) did not find a clear distinction between cationic, neutral and anionic molecules within a different selection of OMPs when investigating the application of Norit SAE Super in hospital wastewater.

Besides electrostatic attraction, a range of further mechanisms that do not occur for neutral compounds can affect the sorption of ionized compounds, including cation bridging, cation- or anion - π bonding, and charge assisted hydrogen bonding (Kah et al., 2017). Other sorbate properties, e.g. molecular weight or the number of atoms in the molecule that have hydrogen donor or acceptor property did not considerably impact OMP sorption (Fig. S 20).

3.4.2. Impact of sorbent properties

High SSA in the range of up to 1000 m^2g^{-1} is a key property of AC (e.g. Hagemann et al., 2018; Marsh and Reinoso, 2006). Activated biochars

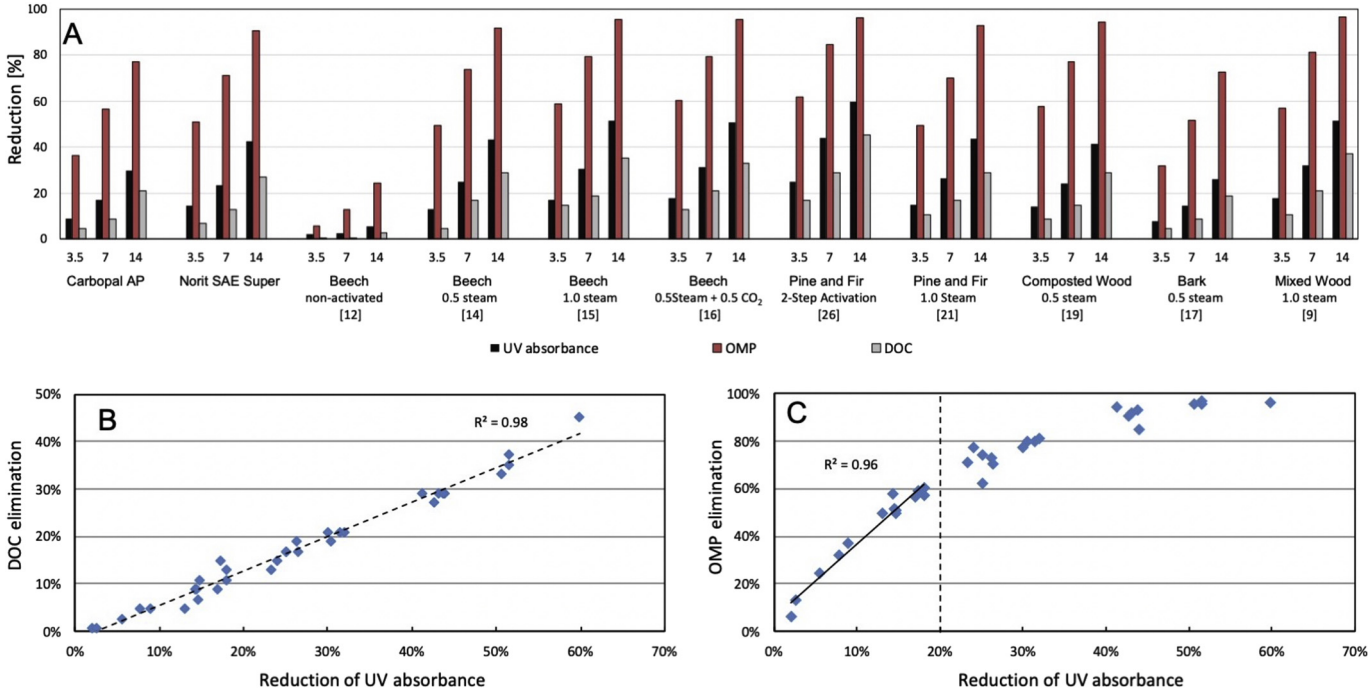

Fig. 3. (A) Reduction of UV absorbance (254 nm), concentration of organic micropollutants (OMP, average reduction of 15 OMPs) and dissolved organic carbon (4.9 mg L^{-1} DOC) in treated wastewater of wastewater treatment plant was Zurich Werdhölzli after shaking for 24 h with 3.5, 7.0 and 14 mg L^{-1} sorbent. Carbopal AP and Norit SAE Super are commercial activated carbons. IDs of sorbents (Table 1) are provided in brackets. Correlation of the reduction of UV absorbance with (B) DOC elimination and (C) OMP elimination for all 33 data points (eleven sorbents and three concentrations).

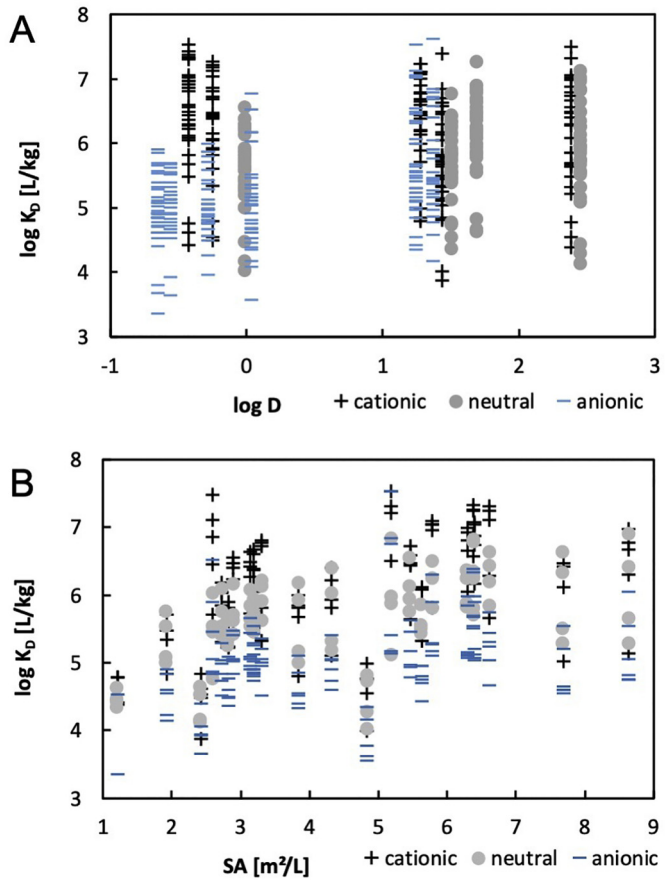

Fig. 4. Mass based distribution coefficients (K_D) of anionic, neutral or cationic organic micropollutants (OMP) as shown in SI Figs. S4–S18. (A) K_D relative to log D of the compounds (cf. Table S4). (B) K_D relative to the available surface area (SA, $m^2\ L^{-1}$), i.e. the BET specific surface area (SSA, $m^2\ g^{-1}$) normalized to the sorbent mass used in batch experiments.

produced in this study showed BET SSAs of 549–1235 m^2g^{-1}. The non-activated, high temperature beech wood biochar had 354 m^2g^{-1} (Table 1), while Carbopal AP and Norit SAE Super had 804 and 912 m^2g^{-1}, respectively. Specific surface area calculated according to other theories or based on CO_2 gas adsorption are shown in the SI (Test S2, Fig. S19). Distribution coefficients based on BET surface area (K_{SA}, L m^{-1}, Fig. S21) indicate that most sorbent surfaces had similar sorption affinities. Thus, sorption generally was higher with higher surface area (Fig. 4B), which confirms that BET SSA is a useful indicator of a pyrogenic sorbent's suitability for OMP sorption.

As discussed above, within our selection of 15 OMPs we found overall higher affinities for cationic OMPs to AC/AB than for neutral OMPs and lowest affinities for anionic OMPs when these compounds have a low hydrophobicity (Fig. 4). This effect could be explained by the ζ potential of AC and AB particles measured in the matrix, i.e. treated wastewater, which was negative and very similar for all sorbents, ranging from −10.0 ± 2.4 mV to −7.8 ± 1.0 mV (Table S3). In ultrapure water, the ζ potential of the particles remaining in suspension ranged from −22.77 ± 0.70 mV to −11.73 ± 0.85 mV (Table S3). However, in treated wastewater, the high similarity in measured ζ potential can be explained by DOC from the wastewater matrix masking the inherent surface charge of the AC and AB particles due to partial surface coverage of the sorbents. Thus, in the wastewater matrix used in this study, potential differences in AC/AB ζ potential apparently did not affect OMP sorption. Similar to the organic coating found on biochars aged in environments rich in DOC (soil, compost, Hagemann et al., 2017), sorption of OMP (or nutrients, Hagemann et al., 2017) on carbonaceous surfaces seems to be at least partially mediated through DOC sorbed from the matrix. Also the ζ potential of nanoparticles in the environment was shown to be determined by sorbed DOC (Chekli et al., 2013; Romanello and de Cortalezzi, 2013).

Average particle size of both AC and AB was similar for all eleven sorbents tested in treated wastewater. Volume based median diameter was ranging from 17.3 ± 0.6 μm to 33.1 ± 6.7 μm (Table S3). Thus, we expect that particle size was not a decisive parameter to explain differences in OMP sorption.

3.4.3. Testing models to predict OMP sorption

Two pp-LFER developed for neutral compounds and AC (Kamlet et al., 1985; Poole and Poole, 1997) were applied for the four compounds predominantly neutral under the experimental conditions (5-methylbenzotriazol, benzotriazole, carbamazepine, and hydrochlorothiazide). However, the models could not predict the experimental data at all (see Fig. S22). The bad performance of these models can partially be explained by a lack of sorbent specific parameterization in the predictive models.

A simpler model based on the pH dependent lipophilicity proxy log D for the sorbate and the BET specific surface area for the sorbent was used to estimate the sorption of acidic and neutral compounds to carbonized materials (Sigmund et al., 2016). The resulting prediction was, irrespective of sorbate speciation, in much better agreement with the trends observed (Fig. S22), however, could not sufficiently reflect differences between compounds and generally underestimated sorption.

4. Conclusion

In this study we systematically tested pyrolysis and activation parameters for the production of AB from low cost, renewable and local sources to replace AC from fossil precursors in advanced WWT. We showed that wood-based ABs exhibited similar or better DOC and OMP elimination as commercial AC. Hence, we can accept our hypothesis that AB from these resources can remove OMPs to the same or higher extent as commercially available AC. We showed that the conditions of physical activation had a higher impact on elimination capacity of wood-based AB than the quality of wood used for their production. Further, the correct dosage of oxidizing agents for physical activation (steam, CO_2 and/or air) needs to be carefully determined and should be reported in the literature on physical activation of carbonaceous materials to allow systematic comparisons between studies.

Sorption of OMP to AC and AB was mainly determined by sorbate's lipophilicity, while the speciation only played a role for OMPs with low hydrophobicity (log D < 1). Looking at sorbents, BET SSA may to some extent indicate the suitability of a carbonaceous material for OMP sorption. However, OMP sorption is matrix dependent, as wastewater DOC may overshadow sorbent's surface properties as e.g. shown for the zeta potential in our study.

To upscale the production of AB for wastewater treatment, contaminants in both AB and commercial AC need to be evaluated thoroughly. Also, economic aspects need to be considered carefully. Our study showed that AB can be produced e.g. from waste timber or woody sieving residues from composting whose disposal would otherwise cause substantial gate fees. However, costs for necessary pre-treatments like drying, shredding, removal of impurities, and homogenization of feedstock must be assessed specifically for each site and feedstock.

CRediT authorship contribution statement

Nikolas Hagemann: Investigation, Writing - original draft, Project administration. **Hans-Peter Schmidt:** Conceptualization, Funding acquisition, Writing - review & editing. **Ralf Kägi:** Funding acquisition, Writing - review & editing. **Marc Böhler:** Funding acquisition, Methodology, Writing - review & editing. **Gabriel Sigmund:** Investigation, Formal analysis, Writing - review & editing. **Andreas Maccagnan:**

Investigation. **Christa S. McArdell:** Methodology, Formal analysis, Writing - review & editing. **Thomas D. Bucheli:** Conceptualization, Funding acquisition, Formal analysis, Writing - review & editing.

Declaration of competing interest

The authors declare that they have no known competing financial interests or personal relationships that could have appeared to influence the work reported in this paper.

Acknowledgements

This research was funded by the Swiss Federal Office for the Environment (BAFU/FOEN). We thank Franziska Blum, Robin Giger, Jens Leifeld, Martin Zuber, Diane Bürge, Johanna Keita and Inge Stockinger for their support in the labs of Agroscope, Severin Neukom and Hans-Peter Müller for technical support and maintenance of PYREKA at Agroscope and Julian Fleiner for support with DOC measurements at Eawag. We acknowledge the support of André Wullschleger and Christian Abegglen at WWTP Zurich Werdhölzli as well as Aline Meier and Pascal Wunderlin of VSA. We thank ZürichHolz AG and Oberland Energie AG for supplying different qualities of wood.

Appendix A. Supplementary data

Supplementary data to this article can be found online at https://doi.org/10.1016/j.scitotenv.2020.138417.

References

ACC Activated Carbon Consortium, 2018a. Activated carbon - high density skeleton. last accessed March 10, 2018. http://www.reachactivatedcarbon.eu/achigh.html.

ACC Activated Carbon Consortium, 2018. Activated carbon - low density skeleton. last accessed March 10, 2018. http://www.reachactivatedcarbon.eu/aclow.html.

Bachmann, H.J., Bucheli, T.D., Dieguez-Alonso, A., Fabbri, D., Knicker, H., Schmidt, H.-P., Ulbricht, A., Becker, R., Buscaroli, A., Buerge, D., Cross, A., Dickinson, D., Enders, A., Esteves, V.I., Evangelou, M.W.H., Fellet, G., Friedrich, K., Gasco Guerrero, G., Glaser, B., Hanke, U.M., Hanley, K., Hilber, I., Kalderis, D., Leifeld, J., Masek, O., Mumme, J., Paneque Carmona, M., Pereira, R.C., Rees, F., Rombola, A.G., Maria de la Rosa, J., Sakrabani, R., Sohi, S., Soja, G., Valagussa, M., Verheijen, F., Zehetner, F., 2016. Toward the standardization of biochar analysis: the COST action TD1107 interlaboratory comparison. J. Agric. Food Chem. 64 (2). https://doi.org/10.1021/acs.jafc.5b05055, 513-527.

Barbosa, M.O., Moreira, N.F.F., Ribeiro, A.R., Pereira, M.F.R., Silva, A.M.T., 2016. Occurrence and removal of organic micropollutants: an overview of the watch list of EU decision 2015/495. Water Res. 94, 257–279. https://doi.org/10.1016/j.watres.2016.02.047.

Baum, S., Pöhler, E., Seubert Hunziker, H., Weber, P., Albisetti, K., Doris, A., 2001. Holzkunde II, 10.3929/ethz-a-004536640. ETH Zurich Research Collection.

Bhatnagar, A., Hogland, W., Marques, M., Sillanpää, M., 2013. An overview of the modification methods of activated carbon for its water treatment applications. Chem. Eng. J. 219, 499–511. https://doi.org/10.1016/j.cej.2012.12.038.

Boehler, M., Zwickenpflug, B., Hollender, J., Ternes, T., Joss, A., Siegrist, H., 2012. Removal of micropollutants in municipal wastewater treatment plants by powder-activated carbon. Water Sci. Technol. 66 (10), 2115–2121. https://doi.org/10.2166/wst.2012.353.

Böhler, M., 2019. Laborversuche zur Bestimmung der Reinigungsleistung von Pulveraktivkohle zur Entfernung von Mikroverunreinigungen auf Kläranlagen - Anleitung. VSA and Eawag last accessed March 10. www.micropoll.ch.

Bourgin, M., Beck, B., Boehler, M., Borowska, E., Fleiner, J., Salhi, E., Teichler, R., von Gunten, U., Siegrist, H., McArdell, C.S., 2018. Evaluation of a full-scale wastewater, treatment plant upgraded with ozonation and biological post-treatments: abatement of micropollutants, formation of transformation products and oxidation by-products. Water Res. 129, 486–498. https://doi.org/10.1016/j.watres.2017.10.036.

Brunauer, S., Emmett, P.H., Teller, E., 1938. Adsorption of gases in multimolecular layers. J. Am. Chem. Soc. 60 (2), 309–319. https://doi.org/10.1021/ja01269a023.

Buss, W., Jansson, S., Masek, O., 2019. Unexplored potential of novel biochar-ash composites for use as organo-mineral fertilizers. J. Clean. Prod. 208, 960–967. https://doi.org/10.1016/j.jclepro.2018.10.189.

Cagnon, B., Py, X., Guillot, A., Stoeckli, F., 2003. The effect of the carbonization/activation procedure on the microporous texture of the subsequent chars and active carbons. Microporous Mesoporous Mater. 57 (3), 273–282. https://doi.org/10.1016/S1387-1811(02)00597-8.

Cao, N., Darmstadt, H., Roy, C., 2001. Activated carbon produced from charcoal obtained by vacuum pyrolysis of softwood bark residues. Energy Fuel 15 (5), 1263–1269. https://doi.org/10.1021/ef0100698.

Chekli, L., Phuntsho, S., Roy, M., Lombi, E., Donner, E., Shon, H.K., 2013. Assessing the aggregation behaviour of iron oxide nanoparticles under relevant environmental conditions using a multi-method approach. Water Res. 47 (13), 4585–4599. https://doi.org/10.1016/j.watres.2013.04.029.

Cornelissen, G., Pandit, N.R., Taylor, P., Pandit, B.H., Sparrevik, M., Schmidt, H.P., 2016. Emissions and char quality of flame-curtain "Kon-Tiki" kilns for farmer-scale charcoal/biochar production. PLoS One 11 (5), e0154617. https://doi.org/10.1371/journal.pone.0154617.

Daughton, C.G., Ruhoy, I.S., 2009. Environmental footprint of pharmaceuticals: the significance of factors beyond direct excretion to sewers. Environ. Toxicol. Chem. 28 (12), 2495–2521. https://doi.org/10.1897/08-382.1.

Devi, P., Saroha, A.K., 2017. Utilization of sludge based adsorbents for the removal of various pollutants: a review. Sci. Total Environ. 578, 16–33. https://doi.org/10.1016/j.scitotenv.2016.10.220.

Dias, J.M., Alvim-Ferraz, M.C.M., Almeida, M.F., Rivera-Utrilla, J., Sanchez-Polo, M., 2007. Waste materials for activated carbon preparation and its use in aqueous-phase treatment: a review. J. Environ. Manag. 85 (4), 833–846. https://doi.org/10.1016/j.jenvman.2007.07.031.

Dobbs, R.A., Wise, R.H., Dean, R.B., 1972. The use of ultra-violet absorbance for monitoring the total organic carbon content of water and wastewater. Water Res. 6 (10), 1173–1180. https://doi.org/10.1016/0043-1354(72)90017-6.

DWA, 2016. Aktivkohleeinsatz auf kommunalen Kläranlagen zur Spurenstoffentfernung – Arbeitsbericht der DWA-Arbeitsgruppe KA-8.6 "Aktivkohleeinsatz auf Kläranlagen". Korrespondenz Abwasser, Abfall 63 (12), 1062–1067.

DWA, 2020. Micropollutants Competence Centre Baden-Württemberg. https://koms-bw.de/en/ last accessed March 5, 2020. Deutsche Vereinigung für Wasserwirtschaft, Abwasser und Abfall (DWA).

Erni, M., Thees, O., Lemm, R., 2017. Altholzpotenziale der Schweiz für die energetische Nutzung. WSL Berichte, p. 5269.

Evers, M., Lange, R.-L., Jagemann, P., Teichgräber, B., Heinz, E., Lübken, M., Wichern, M., 2017. Vergleichende Untersuchungen zur Direktdosierung und nachgeschalteten Dosierung von Pulveraktivkohle. Korrespondenz Abwasser, Abfall 64 (12), 10 (3242/kae2017.12.002, 1067-1073).

Fu, K., Yue, Q., Gao, B., Sun, Y., Zhu, L., 2013. Preparation, characterization and application of lignin-based activated carbon from black liquor lignin by steam activation. Chem. Eng. J. 228, 1074–1082. https://doi.org/10.1016/j.cej.2013.05.028.

Götz, C., Otto, J., Singer, H., 2015. Überprüfung des Reinigungseffekts. Aqua & Gas (2), 34–40.

Gross, M.Y., Maycock, D.S., Thorndyke, M.C., Morritt, D., Crane, M., 2001. Abnormalities in sexual development of the amphipod Gammarus pulex (L.) found below sewage treatment works. Environ. Toxicol. Chem. 20 (8), 1792–1797. https://doi.org/10.1002/etc.5620200824.

Hagemann, N., Joseph, S., Schmidt, H.P., Kammann, C.I., Harter, J., Borch, T., Young, R.B., Varga, K., Taherymoosavi, S., Elliott, K.W., McKenna, A., Albu, M., Mayrhofer, C., Obst, M., Conte, P., Dieguez-Alonso, A., Orsetti, S., Subdiaga, E., Behrens, S., Kappler, A., 2017. Organic coating on biochar explains its nutrient retention and stimulation of soil fertility. Nat. Commun. 8. https://doi.org/10.1038/s41467-017-01123-0.

Hagemann, N., Spokas, K., Schmidt, H.-P., Kägi, R., Böhler, M.A., Bucheli, T.D., 2018. Activated carbon, biochar and charcoal: linkages and synergies across pyrogenic carbon's ABCs. Water 10 (2), 182. https://doi.org/10.3390/w10020182.

Hoeger, B., Köllner, B., Dietrich, D.R., Hitzfeld, B., 2005. Water-borne diclofenac affects kidney and gill integrity and selected immune parameters in brown trout (Salmo trutta f. fario). Aquat. Toxicol. 75 (1), 53–64. https://doi.org/10.1016/j.aquatox.2005.07.006.

Huber, M.B. (2010) Gasifier - Patent DE102007012452B4.

Ioannidou, O., Zabaniotou, A., 2007. Agricultural residues as precursors for activated carbon production - a review. Renew. Sust. Energ. Rev. 11 (9), 1966–2005. https://doi.org/10.1016/j.rser.2006.03.013.

Kah, M., Sigmund, G., Xiao, F., Hofmann, T., 2017. Sorption of ionizable and ionic organic compounds to biochar, activated carbon and other carbonaceous materials. Water Res., 124673–124692 https://doi.org/10.1016/j.watres.2017.07.070.

Kamlet, M.J., Doherty, R.M., Abraham, M.H., Taft, R.W., 1985. Linear solvation energy relationships. 33. An analysis of the factors that influence adsorption of organic-compounds on activated carbon. Carbon 23 (5), 549–554. https://doi.org/10.1016/0008-6223(85)90091-0.

Kim, D.-W., Kil, H.-S., Nakabayashi, K., Yoon, S.-H., Miyawaki, J., 2017. Structural elucidation of physical and chemical activation mechanisms based on the microdomain structure model. Carbon 114, 98–105. https://doi.org/10.1016/j.carbon.2016.11.082.

Kleen, M., Gellerstedt, G., 1995. Influence of inorganic species on the formation of polysaccharide and lignin degradation products in the analytical pyrolysis of pulps. J. Anal. Appl. Pyrolysis 35, 15–41. https://doi.org/10.1016/0165-2370(95)00893-J.

Kong, J., Yue, Q., Huang, L., Gao, Y., Sun, Y., Gao, B., Li, Q., Wang, Y., 2013. Preparation, characterization and evaluation of adsorptive properties of leather waste based activated carbon via physical and chemical activation. Chem. Eng. J. 221, 62–71. https://doi.org/10.1016/j.cej.2013.02.021.

Kovalova, L., Siegrist, H., von Gunten, U., Eugster, J., Hagenbuch, M., Wittmer, A., Moser, R., McArdell, C.S., 2013. Elimination of micropollutants during post-treatment of hospital wastewater with powdered activated carbon, ozone, and UV. Environ. Sci. Technol. 47 (14), 7899–7908. https://doi.org/10.1021/es400708w.

Krull, E.S., Baldock, J.A., Skjemstad, J.O., Smernik, R.J., 2009. In: Lehmann, J., Joseph, S. (Eds.), Biochar for Environmental Management: Science and Technology. Earthscan, London, pp. 53–65.

LfU, 2020. Bayerisches Landesamt für Umwelt, 2009. Merkblatt Verwertung und Beseitigung von Holzaschen. last accessed March 10. https://www.lfl.bayern.de/mam/cms07/iab/dateien/merkblatt_aschen.pdf.

Marsh, H., Reinoso, F.R., 2006. Activated Carbon. Elsevier Science, p. 554.

Masek, O., Buss, W., Brownsort, P., Rovere, M., Tagliaferro, A., Zhao, L., Cao, X.D., Xu, G.W., 2019. Potassium doping increases biochar carbon sequestration potential by 45%,

facilitating decoupling of carbon sequestration from soil improvement. Sci. Rep. 9. https://doi.org/10.1038/s41598-019-41953-0.
Nair, V., Vinu, R., 2016. Peroxide-assisted microwave activation of pyrolysis char for adsorption of dyes from wastewater. Bioresour. Technol. 216, 511–519. https://doi.org/10.1016/j.biortech.2016.05.070.
Poole, S.K., Poole, C.F., 1997. Retention of neutral organic compounds from solution on carbon adsorbents. Anal. Commun. 34 (9), 247–251. https://doi.org/10.1039/A704177B.
Rogowska, J., Cieszynska-Semenowicz, M., Ratajczyk, W., Wolska, L., 2020. Micropollutants in treated wastewater. Ambio 49 (2), 487–503. https://doi.org/10.1007/s13280-019-01219-5.
Romanello, M.B., de Cortalezzi, M.M.F., 2013. An experimental study on the aggregation of TiO2 nanoparticles under environmentally relevant conditions. Water Res. 47 (12), 3887–3898. https://doi.org/10.1016/j.watres.2012.11.061.
Schmidt, H., Taylor, P., 2014. Kon-Tiki flame curtain pyrolysis for the democratization of biochar production. Biochar J 114–124.
Schwarzenbach, R.P., Gschwend, P.M., Imboden, D.M., 2017. Environmental Organic Chemistry. John Wiley & Sons, p. 1024.
Sigmund, G., Sun, H.C., Hofmann, T., Kah, M., 2016. Predicting the sorption of aromatic acids to noncarbonized and carbonized sorbents. Environ. Sci. Technol. 50 (7), 3641–3648. https://doi.org/10.1021/acs.est.5b06033.
Sigmund, G., Hüffer, T., Hofmann, T., Kah, M., 2017. Biochar total surface area and total pore volume determined by N2 and CO2 physisorption are strongly influenced by degassing temperature. Sci. Total Environ. 580, 770–775. https://doi.org/10.1016/j.scitotenv.2016.12.023.
Sørmo, E., Silvani, L., Thune, G., Gerber, H., Schmidt, H.P., Smebye, A.B., Cornelissen, G., 2020. Waste timber pyrolysis in a medium-scale unit: emission budgets and biochar quality. Sci. Total Environ. 718, 137335. https://doi.org/10.1016/j.scitotenv.2020.137335.
Sudhakaran, S., Lattemann, S., Amy, G.L., 2013. Appropriate drinking water treatment processes for organic micropollutants removal based on experimental and model studies — a multi-criteria analysis study. Sci. Total Environ. 442, 478–488. https://doi.org/10.1016/j.scitotenv.2012.09.076.
Sun, Q., Lv, M., Hu, A., Yang, X., Yu, C.P., 2014. Seasonal variation in the occurrence and removal of pharmaceuticals and personal care products in a wastewater treatment plant in Xiamen, China. J. Hazard. Mater. 277, 69–75. https://doi.org/10.1016/j.jhazmat.2013.11.056.
Tan, X.F., Liu, S.B., Liu, Y.G., Gu, Y.L., Zeng, G.M., Hu, X.J., Wang, X., Liu, S.H., Jiang, L.H., 2017. Biochar as potential sustainable precursors for activated carbon production: multiple applications in environmental protection and energy storage. Bioresour. Technol. 227, 359–372. https://doi.org/10.1016/j.biortech.2016.12.083.
Ulrich, N., Endo, S., Brown, T.N., Watanabe, N., Bronner, G., Abraham, M.H., Goss, K.-U., 2017. UFZ-LSER database v 3.2.1. Helmholtz Centre for Environmental Research - UFZ Leipzig last accesed. Jan 7,. 2020. http://www.ufz.de/lserd.
Vogel, H.-J., Baur, S., Triebskorn, R., Rößler, A., Metzger, S., 2014. Die Kläranlage Albstadt-Ebingen: 20 Jahre Pulveraktivkohleeinsatz im Vollstrom. Korrespondenz Abwasser, Abfall 61 (10). https://doi.org/10.3242/kae2014.10.005.
Wan, Z., Sun, Y., Tsang, D.C.W., Yu, I.K.M., Fan, J., Clark, J.H., Zhou, Y., Cao, X., Gao, B., Ok, Y.S., 2019. A sustainable biochar catalyst synergized with copper heteroatoms and CO2 for singlet oxygenation and electron transfer routes. Green Chem. 21 (17), 4800–4814. https://doi.org/10.1039/c9gc01843c.
Wong, S., Ngadi, N., Inuwa, I.M., Hassan, O., 2018. Recent advances in applications of activated carbon from biowaste for wastewater treatment: a short review. J. Clean. Prod. 175, 361–375. https://doi.org/10.1016/j.jclepro.2017.12.059.
Xiao, F., Pignatello, J.J., 2016. Effects of post-pyrolysis air oxidation of biomass chars on adsorption of neutral and Ionizable compounds. Environ. Sci. Technol. 50 (12), 6276–6283. https://doi.org/10.1021/acs.est.6b00362.
Xu, G., Yang, X., Spinosa, L., 2015. Development of sludge-based adsorbents: preparation, characterization, utilization and its feasibility assessment. J. Environ. Manag. 151, 221–232. https://doi.org/10.1016/j.jenvman.2014.08.001.
Yang, K., Peng, J., Xia, H., Zhang, L., Srinivasakannan, C., Guo, S., 2010. Textural characteristics of activated carbon by single step CO2 activation from coconut shells. J. Taiwan Inst. Chem. Eng. 41 (3), 367–372. https://doi.org/10.1016/j.jtice.2009.09.004.
Yu, I.K.M., Xiong, X., Tsang, D.C.W., Wang, L., Hunt, A.J., Song, H., Shang, J., Ok, Y.S., Poon, C.S., 2019. Aluminium-biochar composites as sustainable heterogeneous catalysts for glucose isomerisation in a biorefinery. Green Chem. 21 (6), 1267–1281. https://doi.org/10.1039/c8gc02466a.
Zhang, Y., Geissen, S.U., Gal, C., 2008. Carbamazepine and diclofenac: removal in wastewater treatment plants and occurrence in water bodies. Chemosphere 73 (8), 1151–1161. https://doi.org/10.1016/j.chemosphere.2008.07.086.
Zhang, Y.J., Xing, Z.J., Duan, Z.K., Li, M., Wang, Y., 2014. Effects of steam activation on the pore structure and surface chemistry of activated carbon derived from bamboo waste. Appl. Surf. Sci. 315, 279–286. https://doi.org/10.1016/j.apsusc.2014.07.126.
Zietzschmann, F., Altmann, J., Ruhl, A.S., Dunnbier, U., Dommisch, I., Sperlich, A., Meinel, F., Jekel, M., 2014. Estimating organic micro-pollutant removal potential of activated carbons using UV absorption and carbon characteristics. Water Res. 56, 48–55. https://doi.org/10.1016/j.watres.2014.02.044.